BioArchitecture 3:1, 2–12; January/February 2013; © 2013 Landes Bioscience

Rotary ATPases

Models, machine elements and technical specifications

Alastair G. Stewart,[1,2] Meghna Sobti,[1] Richard P. Harvey[1,2] and Daniela Stock[1,2,*]

[1]The Victor Chang Cardiac Research Institute; Sydney, NSW, Australia; [2]Faculty of Medicine; The University of New South Wales; Sydney, NSW, Australia

Keywords: biological motors, rotary motors, energy conversion, ATP synthase, vacuolar ATPase, A-type ATPase, structural biology, X-ray crystallography, electron microscopy

Rotary ATPases are molecular rotary motors involved in biological energy conversion. They either synthesize or hydrolyze the universal biological energy carrier adenosine triphosphate. Recent work has elucidated the general architecture and subunit compositions of all three subtypes of rotary ATPases. Composite models of the intact F-, V- and A-type ATPases have been constructed by fitting high-resolution X-ray structures of individual subunits or sub-complexes into low-resolution electron densities of the intact enzymes derived from electron cryo-microscopy. Electron cryo-tomography has provided new insights into the supra-molecular arrangement of eukaryotic ATP synthases within mitochondria and mass-spectrometry has started to identify specifically bound lipids presumed to be essential for function. Taken together these molecular snapshots show that nano-scale rotary engines have much in common with basic design principles of man made machines from the function of individual "machine elements" to the requirement of the right "fuel" and "oil" for different types of motors.

Introduction

All living cells require the multifunctional nucleotide adenosine-5'-triphosphate (ATP) both as a carrier of free energy to drive chemical reactions and molecular motion and also as a building block for DNA and RNA. ATP is synthesized in an energetically unfavorable phosphorylation reaction in which inorganic phosphate is added to adenosine-5'-diphosphate (ADP). The majority of the ATP within cells is synthesized by utilizing a trans-membrane gradient of protons or sodium ions generated by either photosynthesis or respiration.[1,2] F-type ATP synthases are trans-membrane molecular rotary motors that perform the final step in these processes by harnessing the membrane potential to synthesize ATP in a rotary catalytic mechanism in a manner similar to the production of electricity in the generators of power plants (**Fig. 1**). The biological conversion of chemical energy within a single glucose molecule via aerobic respiration is a highly optimized process that results in 36 molecules of ATP, whereas the alternative anaerobic pathway, glycolysis, provides only 2 molecules of ATP per glucose molecule. F-type ATPases come in three versions, the eukaryotic ones that reside in the inner membrane of mitochondria, the "powerhouses" of cells, and two simpler versions, the chloroplast and bacterial F-type ATPases that are closely related to each other but have evolved different regulatory mechanisms and subunit stoichiometries to tune them to their environments.[3] Bacterial enzymes have been clocked to run at up to 42,000 rpm under low load, though for intact enzymes under physiological conditions the number is closer to 6000 rpm.[1,4]

Vacuolar or V-type ATPases are more distantly related rotary motors that work in reverse to ATP synthases.[1,5] Using the energy from ATP hydrolysis they pump cations across membranes in a manner similar to man-made rotary pumps. V-type ATPases are important for the acidification of intracellular compartments and generate trans-membrane electrochemical potential gradients that provide the energy for sym- or antiporters to actively transport ions and molecules through membranes. They have been reported to maintain up to 100-fold differences in proton concentration between the cytosol and intracellular compartments. Again there are three versions; the eukaryotic V-type ATPase, and two simpler ones, the bacterial V-type ATPase and the archaeal A-type ATPase, which are structurally indistinguishable and are therefore often summed up as "A-type ATPases/synthases."[1] Many eubacteria and archaea encode only one type of rotary ATPase and whether of F- or A-type these enzymes are thought to be bi-functional in that they can operate in either ATP hydrolysis or synthesis mode depending on cellular requirements (**Fig. 1**).[3,6,7]

All rotary ATPases share an overall conservation of architecture across species and subtypes with a water-soluble $F_1/V_1/A_1$ motor (simplified as R_1 hereafter) and a membrane embedded $F_O/V_O/A_O$ motor (termed R_O hereafter). In intact rotary ATPases R_1 and R_O are connected by two different types of stalks; a central stalk for torque transmission and one to three peripheral stalks for counteracting rotation, stabilization and regulation. Counting the numbers of peripheral stalks is an easy means of rotary ATPase classification: F-type ATPases contain one, prokaryotic A/V-type ATPases contain two and eukaryotic V-type ATPases contain three (**Fig. 1**).[1]

Rotary ATPases consist of 8–15 or more different protein subunits with defined characteristics and functions in analogy to machine elements of the internal combustion engine. Machine

*Correspondence to: Daniela Stock; Email: d.stock@victorchang.edu.au
Submitted: 12/09/12; Accepted: 12/15/12
http://dx.doi.org/10.4161/bioa.23301

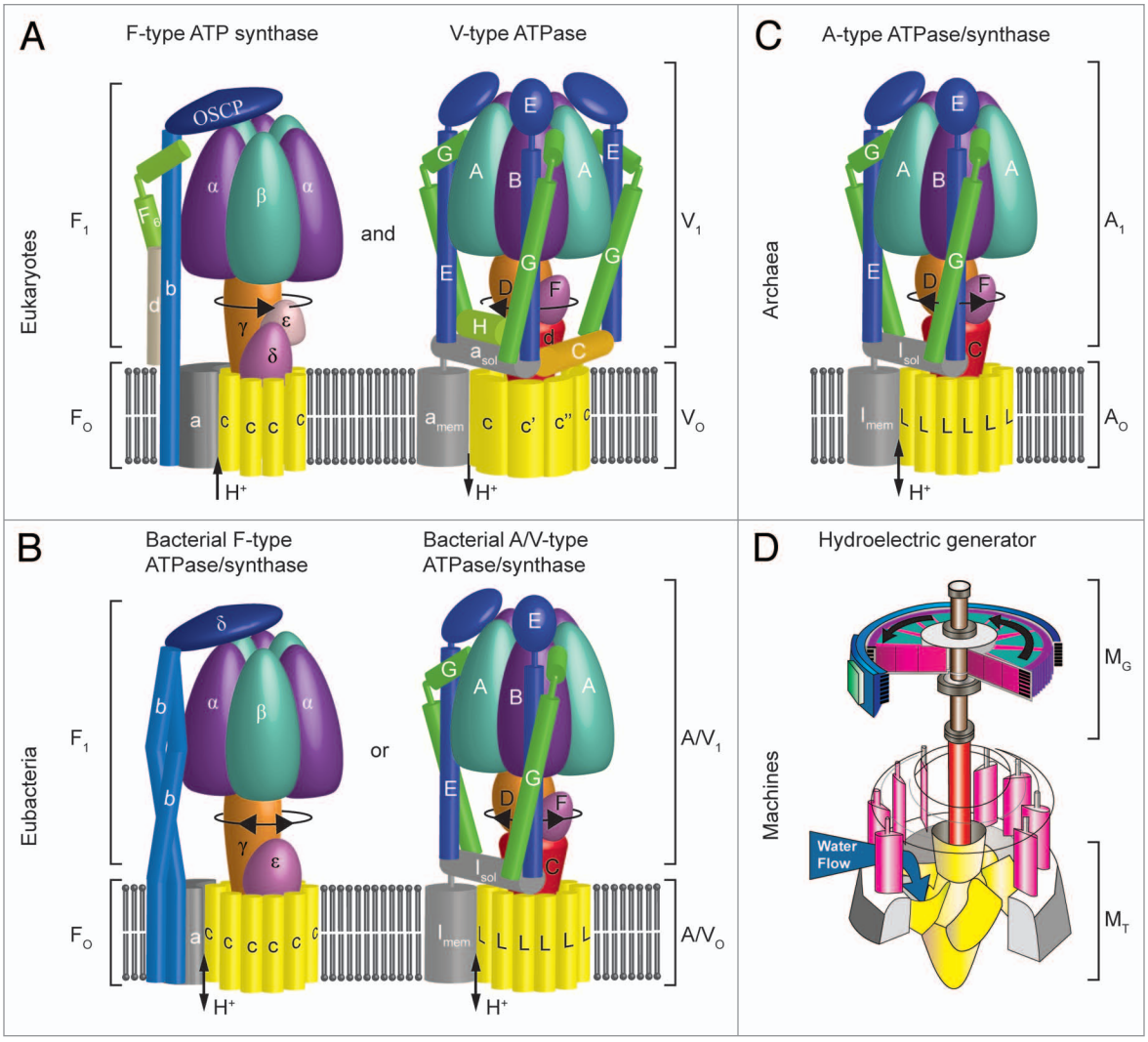

Figure 1. Schematic representations of rotary ATPases across different taxonomic systems. (**A**) Eukaryotes contain two types of rotary ATPases: mitochondrial F_1F_O ATP synthase (left) and vacuolar V_1V_O ATPase (right). (**B**) Many eubacteria have only one rotary ATPase, either bacterial F-type (left) or bacterial A/V-type ATPase/synthase (right), which can operate in either direction. (**C**) Archaea contain A-type ATPases/synthases that are structurally indistinguishable from bacterial A/V-types. (**D**) Comparison to a power generator in a hydroelectric power plant consisting of a turbine (M_T) and an electrical generator (M_G). Adapted from http://en.wikipedia.org/wiki/File:Water_turbine.jpg.

elements, similar to protein subunits are defined as a single piece that cannot be disassembled into a simpler one without destruction, such as a piston, crankshaft or pushrod. The idea of breaking rotary ATPases up into their functional elements, and comparing and contrasting these with the machine elements of a variety of man-made machines will form a major part of this review along with looking at composite models of intact rotary ATPase subtypes and their requirements for specific lipids and fuels.

Different Fuels for Different Motors

All rotary ATPases are comprised of two very different reversible rotary motors that run on different types of fuel: a soluble R_1 motor, which runs on ATP (**Fig. 2**) and a trans-membrane R_O motor, which is powered by a gradient of positively charged ions, usually protons but in some cases sodium ions (**Fig. 3**).[3,8-10] Whether the intact enzyme performs as a chemical generator or as a rotary proton pump depends primarily on the relative concentration of fuels, [protons]: [ATP], in the surrounding medium and on the gear ratio of the rotary ATPase complex as discussed in more detail below.

R_1, The ATP Driven Three-Stroke Motor

High-resolution crystal structures are available for the complete F_1 motor (from "Factor 1," not "Formula 1"!) from several organisms and in several nucleotide-bound states.[11-13] Together with high-resolution single molecule fluorescence studies, which reveal detailed step sizes during catalysis,[14,15] this provides a near-complete atomic resolution movie of ATP hydrolysis, synthesis and the conformational changes in the R_1 motor associated with these chemical reactions. Accordingly, the water-soluble R_1 motors

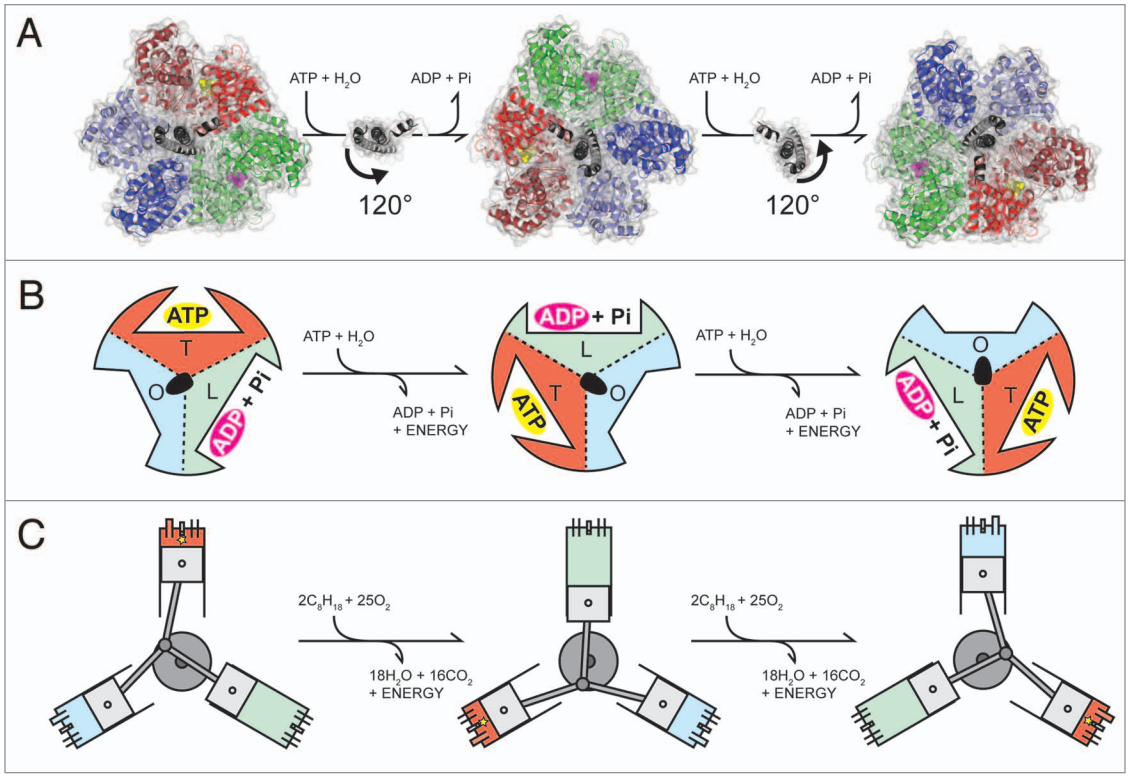

Figure 2. The three-stroke R_1 motor - nucleotide binding and rotary catalysis. (**A**) Three states of the rotary catalytic cycle are captured in the F_1-ATPase structure. Accordingly, the bovine mitochondrial F_1 structure (1COW)[11] is depicted from the "membrane" side in three different orientations: 120° counter-clockwise rotations from left to right indicate the different positions of the central stalk (black) that are related to conformational changes in the nucleotide binding subunits shown as red, green and blue pairs bound to ATP (yellow), ADP/P_i (pink) and unbound, respectively as predicted by P. Boyer's "binding change mechanism"[78] shown in (**B**). The subunits and nucleotide binding modes are depicted in the same colors as the crystal structure and the position of the central stalk is indicated in black (T, tight, ATP bound; L, loose, ADP + Pi bound; O, open, empty). (**C**) Diagram of radial engine rotation in comparison depicted in similar colors.

consist of three pairs of nucleotide binding catalytic and nucleotide binding, but non-catalytic subunits that are arranged around a central stalk with the catalytic site at their interface (**Fig. 2A**). During ATP hydrolysis in the isolated R_1 motor, the nucleotide binding subunits undergo conformational changes, sequentially binding ATP and hydrolysing it to ADP and inorganic phosphate before expelling the products and once again binding ATP (**Fig. 2A and B**). The conformational changes in the nucleotide binding subunits drive a rotation of the central stalk, producing a torque of around 40 pN/nm that can drag long artificially attached actin filaments or large beads through viscous media or drive the rotation of R_O in intact rotary ATPases resulting in the pumping of ions against gradients.[16] As long as there is sufficient supply of fuel (ATP) and no excess of waste-products (ADP), the load on the R_1 motor does not exceed the energy released by hydrolysing three ATP molecules per 360° cycle, the R_1 motor will run in ATP hydrolysis mode and drive a counter-clockwise rotation of the central stalk when viewed from below (**Fig. 2**).[16] The only exception being when regulatory factors, such as inhibitors or inhibitor proteins, are present that prevent rotation in one or both directions.[3] In an intact ATP synthesizing complex, where R_O acts as the motor and R_1 as the chemical generator, the sequence of nucleotide binding and the direction of rotation in the central stalk are reversed. Remarkably, forced clockwise rotation of the central stalk by a mechanical miniature motor acting via magnetic beads attached to the central stalk results in ATP synthesis in R_1.[17]

R_O, The Proton-Driven Rotary Motor

In intact ATP synthases, where the soluble R_1 portion acts as a chemical generator that synthesizes ATP, rotation of the central stalk is driven by the electrochemical potential that drives the flow of protons through the turbine in the R_O motor ("o" for oligomycin binding, not "zero"!) in analogy to gravity driving the flow of water through the turbines of a hydroelectric power plant. Thus, under physiological conditions, the R_O motor needs to be more powerful than the R_1 motor and provide enough power to synthesize three molecules of ATP per 360° cycle. This is dictated by the membrane potential, the turbine stoichiometry (gearing) and the concentration of already synthesized ATP along with regulating mechanisms that can form brakes or ratchets to prevent wasteful hydrolysis of ATP if the membrane potential is low.[3] Due to its membrane location, much less structural information is available for the R_O than for the R_1 motor and hence the molecular details of proton driven rotation are still speculative. In general, all R_O motors consist of a ring of hydrophobic rotor

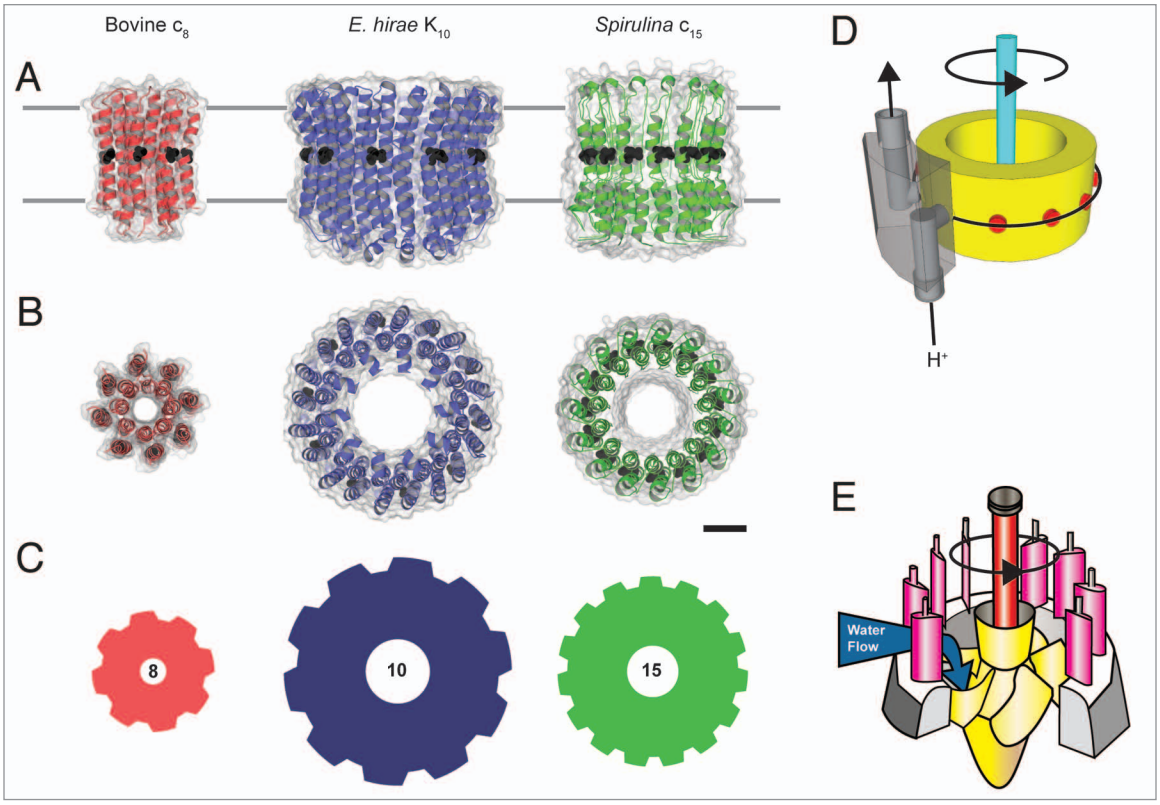

Figure 3. The R_O motor: Different gears for different environments. Ribbon diagrams of bovine c_8 (2XND, red),[21] *E. hirae* K_{10} (2BL2, blue)[33] and *Spirulina* c_{15} (2WIE, green)[79] are shown in (**A**) as side views, and in (**B**) as top views with conserved carboxylate residues shown as black spheres. The scale bar is 20 Å. (**C**) Comparison of rotor rings to a mechanical gear with an equal number of teeth to rotor ring protomers. (**D**) Schematic representation of the R_O motor assembly. The rotor ring is shown in yellow, the stator in gray, protons in red and the central stalk in cyan. Arrows depict flow of protons and direction of rotation. (**E**) Schematic diagram of the turbine in a hydroelectric generator.

subunits that contain conserved, proton binding residues and a single, structurally uncharacterized stator subunit that forms the opposite side of the proton channel (**Fig. 3D**).[18-20]

The Turbines

There is ample structural information about the rotor forming subunits in R_O, historically termed the "proteolipids" due to their hydrophobic character. The rotor rings show a remarkable variation of stoichiometries across species and of the rotary ATPase subtypes so far classified numbers range from 8 to 15 protomers,[21-23] with the notable exception being nine per ring (**Fig. 3**).

F-type ATP synthase rotary subunits consist of single α-helical hairpins that associate into membrane spanning rings.[24] The N-terminal helix is completely hydrophobic and lines a phospholipid-filled cavity impenetrable to charged protons.[20,25,26] The C-terminal helix of each rotor subunit contains a conserved carboxylate residue; this negatively charged residue in the middle of the membrane (colored in black, **Fig. 3**) has been shown to be essential for proton translocation and the generation of torque.[27] V-type ATPases have rotor subunits consisting of two α-helical hairpins that have evolved by gene duplication, but one of the essential carboxylate residues per duplicated subunit is mutated. A-type ATPases have a wide assortment of rotor subunits, ranging from F-type like single hairpins to a whopping 13 fused hairpins in *Methanopyrus kandleri*, presumably forming a 13-meric ring in the intact A-ATPase of this organism.[28]

An Electric Stepping Motor for Protons

The most widely accepted model for proton translocation and the generation of rotation in R_O assumes the presence of two half-channels located at the interface of a structurally unknown trans-membrane subunit and the rotor ring (**Fig. 3D**).[18,20,29,30] According to this model, protons will enter one of the half-channels from the acidic (electropositive) side of the membrane to reach the carboxylate residue in the middle of the membrane. Protonation of this residue neutralizes its negative charge, so it can rotate freely through the hydrophobic membrane. Once it reaches the second half-channel, protons will dissociate from the carboxylate and move toward the more alkaline (electronegative) side of the membrane, thereby exposing the negative charge of the carboxylate residue. The positive charge of a conserved arginine residue in the center of a predicted trans-membrane helix of the stator subunit is believed to attract this charge and capture it during thermal fluctuations, thereby inducing rotation of the ring relative to the membrane and the catalytic subunits in R_1. Incoming protons from the first half-channel will then compete

with the arginine for the negative charge of the carboxylate residue and thereby cause continuous rotation of the ring (**Fig. 3D**).[1]

Rotor Stoichiometry: Gear Ratios

All known R_1 motors have exactly three catalytic sites. As noted above, the rotor rings in R_O isolated from different organisms have been found to contain a wide range of stoichiometries ranging from 8–15 protomers (**Fig. 3A and B**).[23,31] As each rotor subunit generally translocates one proton, rotor stoichiometry relates to the internal proton: ATP ratio of the complex, an important factor that influences the direction and operating mode of rotary ATPases.[6,32] A rotor ring with a larger number of protomers will result in a higher proton: ATP ratio. In this case a larger number of protons are "burnt" in R_O for the production of three ATP molecules in R_1 in each revolution. In the engine analogy, the rotary ATPase with a higher number of protomers has a higher "fuel" (proton) displacement capacity, and is therefore more powerful. Alternatively this could be viewed as a gearing effect, comparable to an engine running in low gear, producing a larger torque (**Fig. 3**). This will enable the corresponding complex to synthesize ATP at smaller membrane potentials and at optimal proton concentrations the displacement effect will produce higher concentrations of ATP than a system with a smaller number of protomers per ring, comparable to an engine in high gear (**Fig. 3**). If the proton: ATP ratio becomes too low, even a very steep ion gradient will not provide enough energy to synthesize three molecules of ATP per revolution at which point the R_1 motor takes over and the complex becomes an ATP fuelled proton pump. This is exactly what happens in V-type ATPases: one of the carboxylate residues in the naturally fused dimers of rotor subunits has been deleted during evolution and while the V-ATPase rotors have large diameters, they contain only halve the number of the proton acceptors, leading to low proton: ATP ratios.[6,33] The number of protomers per ring is therefore an important factor for rotary ATPase performance and the metabolism of a cell.

The Mitochondrial F-Type Super-Engine

Interestingly, vertebrates have the lowest proton to ATP ratio known so far, with only eight rotor subunits per ring, thus "burning" only eight protons for the synthesis of three ATP molecules.[31] This is somewhat puzzling, as some V-type ATPases (i.e., ion pumps running on ATP as a fuel) have been shown to have ten rotor subunits and hence a larger proton: ATP ratio.[33] The explanation might simply be that vertebrate mitochondria have the most sophisticated respiratory system; electron cryo-tomography of mitochondria has revealed that mitochondrial cristae are shaped by lines of dimers of ATP synthases and that other respiratory complexes, such as complexes I to IV, are located in close proximity, forming super-complexes.[34-36] As the other respiratory complexes are responsible for feeding the intermembrane space with protons, having them placed near the vertices of the cristae creates a local maximum of the electro chemical potential (see Strauss et al.[37] for a beautiful explanation of this). This arrangement is akin to a supercharger and allows ATP synthase to function with a much

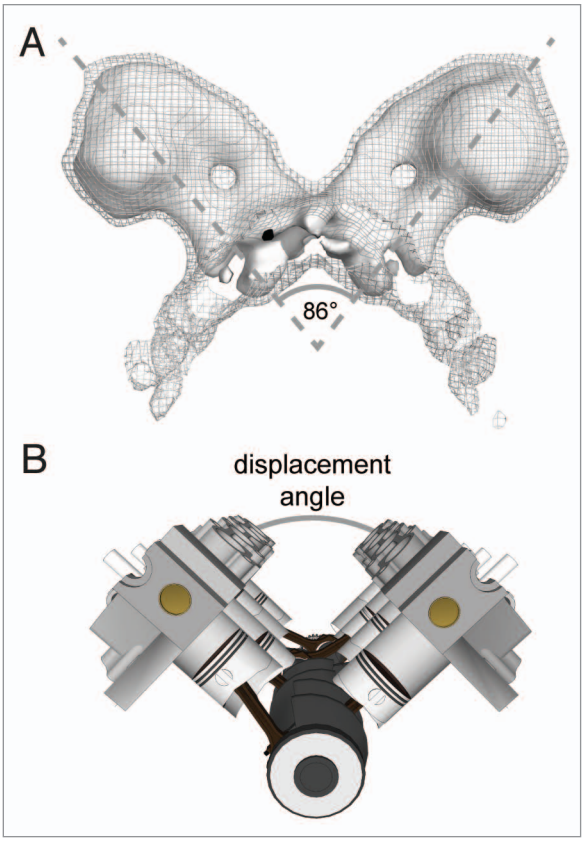

Figure 4. Mitochondrial super-engines. (**A**) Mitochondrial F-type ATP synthase dimers as seen in electron tomograms of frozen intact mitochondria at 37 Å resolution (EMDB code 2161),[66] compared with (**B**) a mechanical V8-engine with lines of four cylinders on either side separated by a 90° displacement angle. Pistons inside the cylinders are coordinated to drive a common crankshaft (adapted from Google SketchUp, Trimble 3D Warehouse).

lower concentration of protons than without cristae. Although the principles of operation are very different, the V-shaped arrays of F-type dimers paradoxically resemble a mechanical V-type motor (**Fig. 4**). Like in different models of mechanical V-type engines, the "displacement angles" of mitochondrial ATP synthase dimers vary depending on species.[34] Values so far range from approximately 90° in yeast mitochondria to close to 180° in potato mitochondria, the latter forming an almost "flat V." As the displacement angle between ATP synthase dimers determines the angle of mitochondrial cristae, which might in turn influence the electrochemical potential gradient across the membrane,[37] this might be an important number to study. The dimerization of mitochondrial F-type ATP synthases may also provide additional anchoring to reduce wasteful rotation of the monomer through the membrane by counteracting rotation of the central stalks. Although it is tempting to speculate that ATP synthase dimers or even rows of dimers rotate in concert, this has never been shown.

Engine Lubrication: Symmetry Mismatch and Lipids

The gear ratio might have further implications; in most known biological rotary motors, the number of protons translocated per

ATP is a non-integral number and hence there is a symmetry mismatch between the R_1 and the R_O ring stoichiometries. This was first described in yeast F-type ATPase,[25] where ten protomers in the R_O motor are related to three catalytic dimers in the R_1 motor. A mismatch leads to a so-called "geometrically frustrated system," where an energy minimum in R_O will never coincide with an energy minimum in R_1, resulting in an "in limbo" system that keeps the motor rotating.[38,39] However, there are notable exceptions among rotary ATPases: The *Thermus thermophilus* A-ATPase R_O motor has 12 protomers[40,41] and the *Spirulina platensis* F-ATPase has 15,[22] both matching the three-fold symmetry in their R_1 motors. This may be possible due to the gearing in these rotary ATPases being much larger, leading to a high proton: ATP ratio and hence a very powerful R_O motor.

R_O motors from different species not only run on different fuels (some preferring sodium ions instead of protons), but also require different phospholipids to function efficiently. Mass spectrometry recently revealed that R_O motors bind specific lipids;[42] the 12 protomers of the *T. thermophilus* rotary ATPase were found to be tightly associated with six phosphatidyl ethanol amine lipids whereas the *E. hirae* bacterial V-type ATPase's ten duplicated subunits are bound to ten bifurcated cardiolipin molecules. These lipids do not represent the predominant lipid species in the host membrane, suggesting that they are specifically filtered from the surrounding membrane. The function of these bound lipids is still unknown, but it is tempting to speculate that they fill gaps in the protein surface that could facilitate a smooth rotation within the membrane. The function of these lipids in rotary ATPases would thus be comparable to oil in an engine, lubricating the moving parts of the motor. It has also been suggested that lipids may stabilize conformations of membrane proteins,[42-44] supported by the array of membrane protein crystal structures that contain bound lipids.[45-49] Given that membrane proteins co-evolved with lipids, it is certainly likely that lipids will influence both membrane protein structure and function.

Central Stalk: The Crankshaft

The general architecture of the central stalk is conserved in all rotary ATPases, being an asymmetric left-handed coiled coil structure that forms a curved "crank."[11] This crank pushes or is pushed by the catalytic subunits depending on the mode of operation. During ATP hydrolysis, the central stalk is akin to the crankshaft of an internal combustion engine, which is pushed by pistons firing within their cylinders (**Fig. 2C**). The rotation of the crankshaft resulting from the torque applied by the pistons can be used to perform work, such as accelerating a car or in the case of rotary ATPases, drive the rotation of R_O that will lead to the pumping of cations against a gradient. The central stalk of rotary ATPases is made of two to three different subunits and connected to the turbine at its base where the rotation is transferred to the rotor ring. The central stalk has been shown to be remarkably flexible by both biophysical experiments[50-52] and several different crystal structures in different conformations.[11-13] It has therefore been hypothesized, that the stalk is able to store elastic energy like a torsion bar in analogy to the suspension of some cars. This energy storage may be able to compensate for multiple protons being pumped for one third of a turn of the R_1 motor, allowing for multiple small steps within the R_O motor for one large (or two sub-) steps within the R_1 motor.

Brakes and Ratchets for the R_1 Motor

Bacterial rotary ATPases have evolved regulatory functions within their small central stalk subunit that can modulate rotary ATPase function; a low-affinity ATP binding site in this subunit allows a switch to proton pumping mode if ATP concentrations are high, but prevents ATP hydrolysis when ATP levels are low.[53] This allows replenishment of proton gradients that also drive the bacterial flagellar motor if there is no shortage of ATP. If ATP levels are low, a conformational change occurs and the subunit intercalates in between the nucleotide binding subunits thus preventing ATP hydrolysis, but still allowing synthesis, just like a ratchet. Eukaryotic F-type ATP synthases are never supposed to run in reverse and have evolved a third central stalk subunit that prevents conformational changes in this regulatory subunit and an additional inhibitor protein termed IF_1 that intercalates with F_1 to prevent ATP hydrolysis under ischemic conditions. In contrast to the bacterial regulatory mechanism, which is ATP-dependent, the mitochondrial IF_1 protein is regulated by pH.[54,55]

Peripheral Stalks: Scaffolds, Torsion Bars and Pushrods

The peripheral stalks are the most divergent elements of rotary ATPases both in sequence and subunit composition, indicating that they may be important for regulation and fine-tuning of the intact complexes. Their primary function is to prevent rotation between the stator components of the R_1 and R_O motors, so that the central stalk and rotor ring are able to rotate relative to the proton channel and catalytic sites.[56] The number of peripheral stalks within the complex has recently been recognized as the hallmark of rotary ATPase classification; all known F-types contain one, A-types contain two and eukaryotic V-types contain three (**Fig. 1**).[1] High-resolution structures of the peripheral stalks from F-, V- and A-type ATPases are now available,[57-59] leaving only the bacterial F-type peripheral stalk structure to be determined. However, it was the sequence analysis of this bacterial F-type peripheral stalk that first revealed an unusual sequence repeat, predicted to form a right-handed coiled coil structure within the homo-dimer of this subunit (**Fig. 1**).[60] Coiled coils are common structural motifs that are formed by one α-helix coiling around another. The coiling almost always occurs in a left-handed fashion, and is encoded by heptad repeats within the sequence of many motor proteins including the central stalk of rotary ATPases as discussed earlier. The heptad repeat refers to a seven residue periodic nature of the sequence, placing apolar residues at position a and d in the $(a\text{-}b\text{-}c\text{-}d\text{-}e\text{-}f\text{-}g)_n$ repeating unit.[61] The left-handed coiled coil's pitch (distance to obtain one full turn) of ~200 Å is caused by the slight mismatch between repeating units of the α-helix (3.6 residues per turn) and the sequence repeats (7/2 or 3.5). Right-handed coiled coils on the other hand

are extremely rare, with only a handful of proteins being identified to contain them.[62,63] They are encoded by either hendecad (11 residue) or quindecad (15 residue) repeats that lead to very different pitches. Hendecad repeats result in virtually parallel helices (with a pitch ~1000 Å), while quindecad repeats produce a similar pitch to that of a left-handed coiled coil (~200 Å) though coiling in the opposite direction.

Comparison of sequences and structures revealed that the general architecture of the peripheral stalks is conserved despite a lack in sequence homology.[58,59,64] They form elongated structures that can be divided into two subcomponents, an R_1 motor binding globular domain and a 140–160 Å long mostly right-handed coiled coil pointing toward R_O. The pitch of the coil is encoded by sequence repeats that dictate flexibility in three dimensions along the length of the structure: The N-terminal half of the coil that points toward the R_O motor contains hendecad repeats leading to almost parallel helices. These span the gap between the R_1 and R_O motors and are positioned such that they are rigid in the direction of rotation, just as a beam is rigid in one direction but flexible in the other, thus preventing rotation between the R_1 and R_O stators. The C-terminal half contains a right-handed coiled coil encoded by a quindecad repeat, which, like left-handed coiled coils is flexible in all directions and can thus compensate for the movements within the R_1 motor during catalysis without breaking and reforming the chemical bonds at the interfaces of these subunits.

Assembling Rotary ATPases From Their Machine Elements

Intact rotary ATPases have been purified from various sources and studied by electron microscopy.[1] The resulting three-dimensional reconstructions provide low-resolution 3D envelopes to assemble composite "pseudo-atomic" models by fitting higher-resolution crystal structures of subunits or sub-complexes. The most accurate model of F-type ATPases obtained in this way is that of the bovine mitochondrial F-type ATP synthase at 18 Å resolution that accommodates all known crystal structures well (**Fig. 5A**).[65] Notably the crystal structure of the bovine peripheral stalk complex requires some bending along similar "hinges" as the A-type peripheral stalk to fit into the electron microscopy density. This suggests that both peripheral stalk complexes have similar dynamic properties, which may be important for the accommodation of conformational changes in the R_1 motor during rotary catalysis. It may also provide a means of cross-talk in between subunits and perhaps also in between mitochondrial F-type ATP synthase dimers. Accurate composite models of these dimers have been obtained by fitting of monomeric models into cryo electron tomograms of intact mitochondria,[66] thus providing a composite model of the ATP synthase dimers in situ.[65,66]

A-type ATPases have been purified from several sources and studied by electron microscopy, providing envelopes of similar shapes all showing two peripheral stalks that are connected to each other at their bases by an N-terminal soluble appendage of the ion channel forming stator subunit (**Figs. 1 and 5B**).[40,67,68] As F-type ATPases have only one peripheral stalk, this structural element akin to a rocker in an engine is not needed and hence is unique to A- and V-type ATPases. The highest resolution image of any intact rotary ATPase to date is that of the 660 kDa A/V-type ATPase isolated from the thermophilic eubacterium *T. thermophilus* at 9.7 Å, allowing very accurate placement of all nine different subunits and provides the most detailed view of the trans-membrane stator subunit (**Fig. 5B**).[68]

V-type ATPases contain three peripheral stalks, held together by a triangular network of connecting subunits at their base, one made of the ion channel appendage, the other being a connector subunit unique to eukaryotic V-type ATPases (**Fig. 1A**).[69] Regulation of eukaryotic V-ATPases is achieved by a reversible dissociation process, where the V_1 motor disengages from the V_O motor to prevent wasteful ATP hydrolysis.[70] This dissociation process has recently been suggested to be facilitated by a "spring loading" mechanism, using the protein RAVE[71] and an even more "bendable" peripheral stalk[59] that can store elastic energy in a bulge seen in the crystal structure of the yeast V-type peripheral stalk complex just below its globular head domain that may act as a spring. Assembly of intact V-ATPases requires the input of energy through the chaperone RAVE through interaction with the unique connector subunit and this results in a strained V-ATPase complex that is able to easily disassemble in response to relatively low-energy stimuli,[59] akin to a catapult or ejector seat mechanism. Although this puts additional challenges on the isolation of intact eukaryotic complexes, 3D electron microscopy reconstructions have been obtained to resolutions of 17 Å and 11 Å from hornworm and yeast V-ATPases respectively (**Fig. 5C**),[72,73] allowing the assembly of fairly accurate composite V-ATPase models. Mammalian V-ATPase subunits have many organelle-specific isoforms[74] that are likely to confer further regulation on assembly, disassembly and performance of these intricate molecular machines thereby fine tuning them to their environment.

There is increasing evidence that rotary ATPases are highly dynamic structures and that each individual element, from the central stalk to the peripheral stalks and the turbines bear a certain degree of flexibility.[30,58,75] This is supported by an apparent inclination of the R_1 relative to the R_O motor observed in class averages of electron micrographs of all rotary ATPase subtypes[40,76] and crystal structures of complexes containing both the R_1 motor and the trans-membrane rotor ring.[21,25,77] The concerted dynamics conferred by the peripheral stalks to different parts of the structure may provide a means of cross-talk between different parts of the complex,[58] so the ion channel in R_O will know what the nucleotide binding domains in R_1 at a distance of greater than 100 Å are doing and vice versa. This works with one peripheral stalk in F-type ATPases, but better with two in A-type ATPases and best in V-type ATPases that have the maximum number of peripheral stalks that are connected at their bases and can thus confer information between all catalytic subunits and the distal side of the ion channel. The idea of cooperativity can be thought of as a camshaft in an internal combustion engine, where information about the position of the pistons is transferred through a gear, belt or pushrod to one or more camshafts, which open the

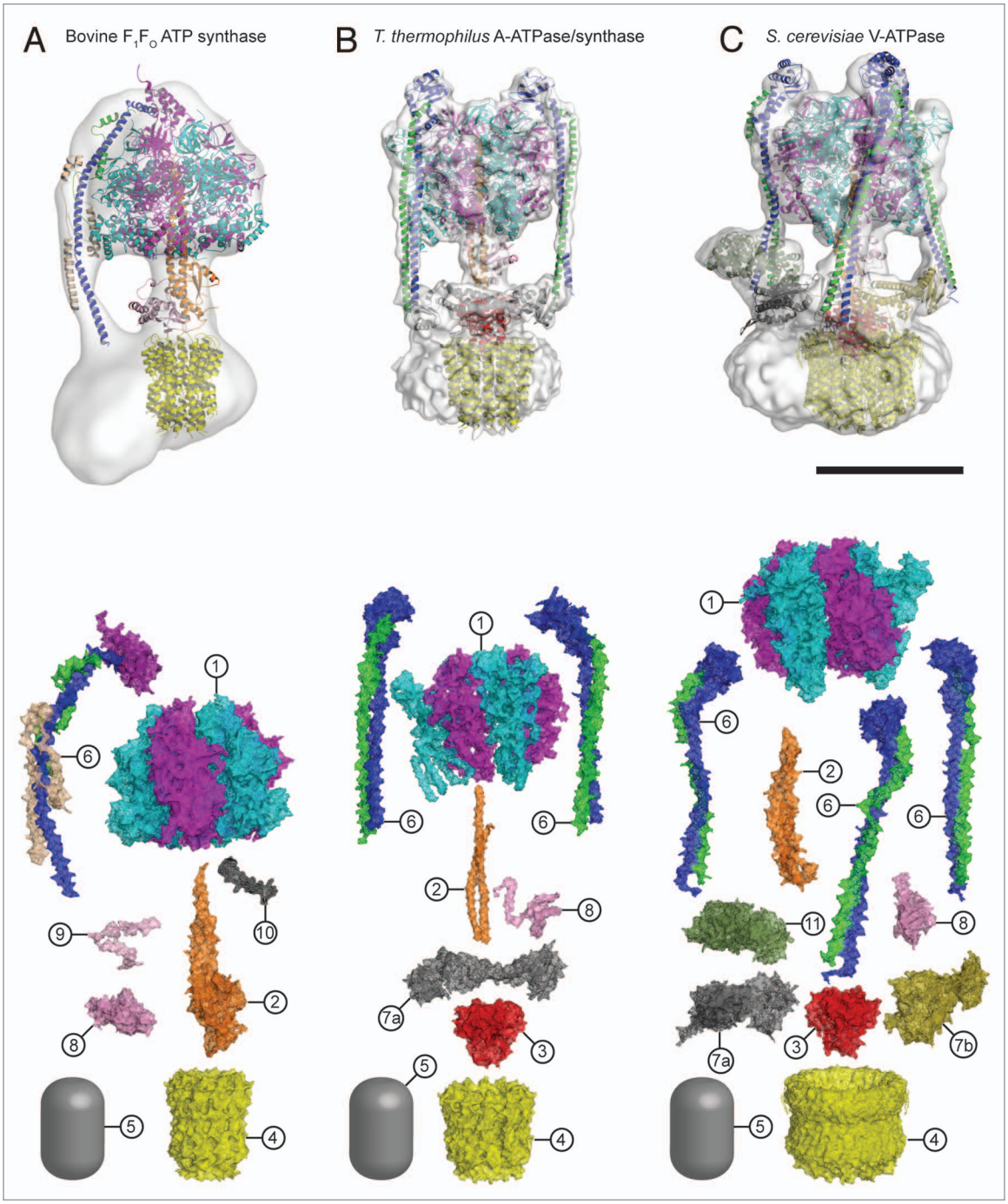

Figure 5. Composite models of rotary ATPase subtypes and their "machine elements." F-, A- and V-type composite models are shown in similar color schemes with electron microscopy densities at 18 Å, 9.7 Å and 11 Å in transparent light gray (EMD IDs 2091, 5335 and 5476 respectively).[65,68,73] Below are "exploded" views depicting individual "machine elements" at higher resolution derived from crystal structures. (**A**) bovine mitochondrial F-type ATP synthase, (**B**) *T. thermophilus* A-type ATPase/synthase, (**C**) yeast V-type ATPase. 1, nucleotide binding stator subunits ("cylinders") (F: 2WPD | A: 3A5C | V: 3A5C); 2, central stalk ("crankshaft") (F: 2WPD | A: 3A5C | V: 3AON); 3, A/V rotor subunit ("adapter") (A: 1R5Z | V: 1R5Z); 4, rotor ring ("turbine") (F: 4B2Q | A: 1C17 | V: 2BL2); 5, ion channel forming subunit (no structure available); 6, peripheral stalk ("pushrod") (F: 4B2Q [2B05/2CLY/2WSS] | A: 3K5B | V: 4DL0 and 4EFA); 7a and b, A/V peripheral stalk connector subunits ("rockers") (A: 3RRK | V: 3RRK and 1U7L); 8, small central stalk subunit ("ratchet" in prokaryotes) (F: 2WPD | A: 3A5C | V: 3AON); 9, eukaryotic additional central stalk subunit ("lock") (2WPD); 10, IF_1 ("brake") (1OHH); 11, eukaryotic V-type additional peripheral stalk subunit ("brake") (1HO8). The scale bar corresponds to 100 Å.

valves and deliver the spark, so that all components of the engine operate in the correct order and with the right timing.

Conclusions

Molecular machines, like the rotary ATPases described here, seem to have much in common with man-made machines. However, the analogies hold only to a certain point and are in large parts not fully understood. What is evident is that several billion years of evolution have resulted in biological motors that are unsurpassed in efficiency, fine-tuning to their environment and sustainability. Understanding their detailed function at the molecular level is not only important to satisfy our curiosity, but will certainly have implications in understanding human physiology, including mitochondrial disorders, bioenergetics and the processes of aging, as well as impacting nano-engineering and many other fields afar.

Disclosure of Potential Conflicts of Interest

No potential conflicts of interest were disclosed.

Acknowledgments

We would like to thank Boris Martinac, Victor Chang Cardiac Research Institute, and James Walsh, School of Physics, University of New South Wales, Australia for critical reading of the manuscript and Stephan Wilkens, Department of Biochemistry and Molecular Biology, State University of New York for providing a composite model of yeast V-type ATPase used in Figure 5C. R.P.H. is funded by grants from the National Health and Medical Research Council of Australia (NHMRC: 573732, 573703) and holds an NHMRC Australia Fellowship (573705). D.S., A.G.S., and M.S. are funded by the National Health and Medical Research Council of Australia (NHMRC: 1022143, 1047004, 1004620) and the Australian Research Council (DP110101387).

References

1. Muench SP, Trinick J, Harrison MA. Structural divergence of the rotary ATPases. Q Rev Biophys 2011; 44:311-56; PMID:21426606; http://dx.doi.org/10.1017/S0033583510000338
2. von Ballmoos C, Wiedenmann A, Dimroth P. Essentials for ATP synthesis by F1F0 ATP synthases. Annu Rev Biochem 2009; 78:649-72; PMID:19489730; http://dx.doi.org/10.1146/annurev.biochem.78.081307.104803
3. von Ballmoos C, Cook GM, Dimroth P. Unique rotary ATP synthase and its biological diversity. Annual review of biophysics 2008; 37:43-64
4. Nakanishi-Matsui M, Kashiwagi S, Hosokawa H, Cipriano DJ, Dunn SD, Wada Y, et al. Stochastic high-speed rotation of Escherichia coli ATP synthase F1 sector: the epsilon subunit-sensitive rotation. J Biol Chem 2006; 281:4126-31; PMID:16352612; http://dx.doi.org/10.1074/jbc.M510090200
5. Forgac M. Vacuolar ATPases: rotary proton pumps in physiology and pathophysiology. Nat Rev Mol Cell Biol 2007; 8:917-29; PMID:17912264; http://dx.doi.org/10.1038/nrm2272
6. Cross RL, Müller V. The evolution of A-, F-, and V-type ATP synthases and ATPases: reversals in function and changes in the H+/ATP coupling ratio. FEBS Lett 2004; 576:1-4; PMID:15473999; http://dx.doi.org/10.1016/j.febslet.2004.08.065
7. Nakano M, Imamura H, Toei M, Tamakoshi M, Yoshida M, Yokoyama K. ATP hydrolysis and synthesis of a rotary motor V-ATPase from Thermus thermophilus. J Biol Chem 2008; 283:20789-96; PMID:18492667; http://dx.doi.org/10.1074/jbc.M801276200
8. Oster G, Wang H. ATP synthase: two motors, two fuels. Structure 1999; 7:R67-72; PMID:10196130; http://dx.doi.org/10.1016/S0969-2126(99)80046-X
9. Krah A, Pogoryelov D, Langer JD, Bond PJ, Meier T, Faraldo-Gomez JD. Structural and energetic basis for H(+) versus Na(+) binding selectivity in ATP synthase F(o) rotors. Bba-Bioenergetics 2010; 1797:763-72
10. Pogoryelov D, Krah A, Langer J, Faraldo-Gomez JD, Meier T. On the rotary mechanism and ion binding specificity of F1Fo-ATP synthases. FEBS J 2010; 277:213
11. Abrahams JP, Leslie AG, Lutter R, Walker JE. Structure at 2.8 A resolution of F1-ATPase from bovine heart mitochondria. Nature 1994; 370:621-8; PMID:8065448; http://dx.doi.org/10.1038/370621a0
12. Okazaki K, Takada S. Structural comparison of F1-ATPase: interplay among enzyme structures, catalysis, and rotations. Structure 2011; 19:588-98; PMID:21481781; http://dx.doi.org/10.1016/j.str.2011.01.013
13. Rees DM, Montgomery MG, Leslie AG, Walker JE. Structural evidence of a new catalytic intermediate in the pathway of ATP hydrolysis by F1-ATPase from bovine heart mitochondria. Proc Natl Acad Sci U S A 2012; 109:11139-43; PMID:22733764; http://dx.doi.org/10.1073/pnas.1207587109
14. Noji H, Yasuda R, Yoshida M, Kinosita K Jr. Direct observation of the rotation of F1-ATPase. Nature 1997; 386:299-302; PMID:9069291; http://dx.doi.org/10.1038/386299a0
15. Adachi K, Oiwa K, Nishizaka T, Furuike S, Noji H, Itoh H, et al. Coupling of rotation and catalysis in F(1)-ATPase revealed by single-molecule imaging and manipulation. Cell 2007; 130:309-21; PMID:17662945; http://dx.doi.org/10.1016/j.cell.2007.05.020
16. Kinosita K Jr., Yasuda R, Noji H, Adachi K. A rotary molecular motor that can work at near 100% efficiency. Philos Trans R Soc Lond B Biol Sci 2000; 355:473-89; PMID:10836501; http://dx.doi.org/10.1098/rstb.2000.0589
17. Itoh H, Takahashi A, Adachi K, Noji H, Yasuda R, Yoshida M, et al. Mechanically driven ATP synthesis by F1-ATPase. Nature 2004; 427:465-8; PMID:14749837; http://dx.doi.org/10.1038/nature02212
18. Vik SB, Antonio BJ. A mechanism of proton translocation by F1F0 ATP synthases suggested by double mutants of the a subunit. J Biol Chem 1994; 269:30364-9; PMID:7982950
19. Hakulinen JK, Klyszejko AL, Hoffmann J, Eckhardt-Strelau L, Brutschy B, Vonck J, et al. Structural study on the architecture of the bacterial ATP synthase Fo motor. Proc Natl Acad Sci U S A 2012; 109:E2050-6; PMID:22736796; http://dx.doi.org/10.1073/pnas.1203971109
20. Pogoryelov D, Krah A, Langer JD, Yildiz O, Faraldo-Gómez JD, Meier T. Microscopic rotary mechanism of ion translocation in the F(o) complex of ATP synthases. Nat Chem Biol 2010; 6:891-9; PMID:20972431; http://dx.doi.org/10.1038/nchembio.457
21. Watt IN, Montgomery MG, Runswick MJ, Leslie AG, Walker JE. Bioenergetic cost of making an adenosine triphosphate molecule in animal mitochondria. Proc Natl Acad Sci U S A 2010; 107:16823-7; PMID:20847295; http://dx.doi.org/10.1073/pnas.1011099107
22. Pogoryelov D, Yu J, Meier T, Vonck J, Dimroth P, Muller DJ. The c15 ring of the Spirulina platensis F-ATP synthase: F1/F0 symmetry mismatch is not obligatory. EMBO Rep 2005; 6:1040-4; PMID:16170308; http://dx.doi.org/10.1038/sj.embor.7400517
23. Pogoryelov D, Reichen C, Klyszejko AL, Brunisholz R, Muller DJ, Dimroth P, et al. The oligomeric state of c rings from cyanobacterial F-ATP synthases varies from 13 to 15. J Bacteriol 2007; 189:5895-902; PMID:17545285; http://dx.doi.org/10.1128/JB.00581-07
24. Girvin ME, Rastogi VK, Abildgaard F, Markley JL, Fillingame RH. Solution structure of the transmembrane H+-transporting subunit c of the F1F0 ATP synthase. Biochemistry 1998; 37:8817-24; PMID:9636021; http://dx.doi.org/10.1021/bi980511m
25. Stock D, Leslie AG, Walker JE. Molecular architecture of the rotary motor in ATP synthase. Science (New York, NY) 1999; 286:1700-5
26. Seelert H, Poetsch A, Dencher NA, Engel A, Stahlberg H, Müller DJ. Structural biology. Proton-powered turbine of a plant motor. Nature 2000; 405:418-9; PMID:10839529; http://dx.doi.org/10.1038/35013148
27. Fillingame RH. Subunit c of F1F0 ATP synthase: structure and role in transmembrane energy transduction. Biochim Biophys Acta 1992; 1101:240-3; PMID:1385981
28. Lolkema JS, Boekema EJ. The A-type ATP synthase subunit K of Methanopyrus kandleri is deduced from its sequence to form a monomeric rotor comprising 13 hairpin domains. FEBS Lett 2003; 543:47-50; PMID:12753903; http://dx.doi.org/10.1016/S0014-5793(03)00398-3
29. Junge W, Lill H, Engelbrecht S. ATP synthase: an electrochemical transducer with rotatory mechanics. Trends Biochem Sci 1997; 22:420-3; PMID:9397682; http://dx.doi.org/10.1016/S0968-0004(97)01129-8
30. Saroussi S, Schushan M, Ben-Tal N, Junge W, Nelson N. Structure and flexibility of the C-ring in the electromotor of rotary F(o)F(1)-ATPase of pea chloroplasts. PLoS One 2012; 7:e43045; PMID:23049735; http://dx.doi.org/10.1371/journal.pone.0043045
31. Watt IN, Montgomery MG, Runswick MJ, Leslie AGW, Walker JE. Bioenergetic cost of making an adenosine triphosphate molecule in animal mitochondria. Proc Natl Acad Sci U S A 2010; 107:16823-7; PMID:20847295; http://dx.doi.org/10.1073/pnas.1011099107

32. Pogoryelov D, Klyszejko AL, Krasnoselska GO, Heller EM, Leone V, Langer JD, et al. Engineering rotor ring stoichiometries in the ATP synthase. Proc Natl Acad Sci U S A 2012; 109:E1599-608; PMID:22628564; http://dx.doi.org/10.1073/pnas.1120027109
33. Murata T, Yamato I, Kakinuma Y, Leslie AGW, Walker JE. Structure of the rotor of the V-type Na+-ATPase from Enterococcus hirae. Science (New York, NY) 2005; 308:654-9
34. Davies KM, Strauss M, Daum B, Kief JH, Osiewacz HD, Rycovska A, et al. Macromolecular organization of ATP synthase and complex I in whole mitochondria. Proc Natl Acad Sci U S A 2011; 108:14121-6; PMID:21836051; http://dx.doi.org/10.1073/pnas.1103621108
35. Dudkina NV, Sunderhaus S, Boekema EJ, Braun HP. The higher level of organization of the oxidative phosphorylation system: mitochondrial supercomplexes. J Bioenerg Biomembr 2008; 40:419-24; PMID:18839290; http://dx.doi.org/10.1007/s10863-008-9167-5
36. Frenzel M, Rommelspacher H, Sugawa MD, Dencher NA. Ageing alters the supramolecular architecture of OxPhos complexes in rat brain cortex. Exp Gerontol 2010; 45:563-72; PMID:20159033; http://dx.doi.org/10.1016/j.exger.2010.02.003
37. Strauss M, Hofhaus G, Schröder RR, Kühlbrandt W. Dimer ribbons of ATP synthase shape the inner mitochondrial membrane. EMBO J 2008; 27:1154-60; PMID:18323778; http://dx.doi.org/10.1038/emboj.2008.35
38. Hendrix RW. Symmetry mismatch and DNA packaging in large bacteriophages. Proc Natl Acad Sci U S A 1978; 75:4779-83; PMID:283391; http://dx.doi.org/10.1073/pnas.75.10.4779
39. Stock D, Gibbons C, Arechaga I, Leslie AG, Walker JE. The rotary mechanism of ATP synthase. Curr Opin Struct Biol 2000; 10:672-9; PMID:11114504; http://dx.doi.org/10.1016/S0959-440X(00)00147-0
40. Bernal RA, Stock D. Three-dimensional structure of the intact Thermus thermophilus H+-ATPase/synthase by electron microscopy. Structure 2004; 12:1789-98; PMID:15458628; http://dx.doi.org/10.1016/j.str.2004.07.017
41. Toei M, Gerle C, Nakano M, Tani K, Gyobu N, Tamakoshi M, et al. Dodecamer rotor ring defines H+/ATP ratio for ATP synthesis of prokaryotic V-ATPase from Thermus thermophilus. Proc Natl Acad Sci U S A 2007; 104:20256-61; PMID:18077374; http://dx.doi.org/10.1073/pnas.0706914105
42. Zhou M, Morgner N, Barrera NP, Politis A, Isaacson SC, Matak-Vinkovic D, et al. Mass spectrometry of intact V-type ATPases reveals bound lipids and the effects of nucleotide binding. Science (New York, NY) 2011; 334:380-5
43. Jiang QX, Gonen T. The influence of lipids on voltage-gated ion channels. Curr Opin Struct Biol 2012; 22:529-36; PMID:22483432; http://dx.doi.org/10.1016/j.sbi.2012.03.009
44. Reichow SL, Gonen T. Lipid-protein interactions probed by electron crystallography. Curr Opin Struct Biol 2009; 19:560-5; PMID:19679462; http://dx.doi.org/10.1016/j.sbi.2009.07.012
45. Vogeley L, Sineshchekov OA, Trivedi VD, Sasaki J, Spudich JL, Luecke H. Anabaena sensory rhodopsin: a photochromic color sensor at 2.0 A. Science (New York, NY) 2004; 306:1390-3
46. Schobert B, Cupp-Vickery J, Hornak V, Smith S, Lanyi J. Crystallographic structure of the K intermediate of bacteriorhodopsin: conservation of free energy after photoisomerization of the retinal. J Mol Biol 2002; 321:715-26; PMID:12206785; http://dx.doi.org/10.1016/S0022-2836(02)00681-2
47. Lange C, Nett JH, Trumpower BL, Hunte C. Specific roles of protein-phospholipid interactions in the yeast cytochrome bc1 complex structure. EMBO J 2001; 20:6591-600; PMID:11726495; http://dx.doi.org/10.1093/emboj/20.23.6591
48. Huang LS, Cobessi D, Tung EY, Berry EA. Binding of the respiratory chain inhibitor antimycin to the mitochondrial bc1 complex: a new crystal structure reveals an altered intramolecular hydrogen-bonding pattern. J Mol Biol 2005; 351:573-97; PMID:16024040; http://dx.doi.org/10.1016/j.jmb.2005.05.053
49. Tsukihara T, Shimokata K, Katayama Y, Shimada H, Muramoto K, Aoyama H, et al. The low-spin heme of cytochrome c oxidase as the driving element of the proton-pumping process. Proc Natl Acad Sci U S A 2003; 100:15304-9; PMID:14673090; http://dx.doi.org/10.1073/pnas.2635097100
50. Wächter A, Bi Y, Dunn SD, Cain BD, Sielaff H, Wintermann F, et al. Two rotary motors in F-ATP synthase are elastically coupled by a flexible rotor and a stiff stator stalk. Proc Natl Acad Sci U S A 2011; 108:3924-9; PMID:21368147; http://dx.doi.org/10.1073/pnas.1011581108
51. Junge W, Sielaff H, Engelbrecht S. Torque generation and elastic power transmission in the rotary F(O)F(1)-ATPase. Nature 2009; 459:364-70; PMID:19458712; http://dx.doi.org/10.1038/nature08145
52. Sielaff H, Rennekamp H, Wächter A, Xie H, Hilbers F, Feldbauer K, et al. Domain compliance and elastic power transmission in rotary F(O)F(1)-ATPase. Proc Natl Acad Sci U S A 2008; 105:17760-5; PMID:19001275; http://dx.doi.org/10.1073/pnas.0807683105
53. Yagi H, Kajiwara N, Tanaka H, Tsukihara T, Kato-Yamada Y, Yoshida M, et al. Structures of the thermophilic F1-ATPase epsilon subunit suggesting ATP-regulated arm motion of its C-terminal domain in F1. Proc Natl Acad Sci U S A 2007; 104:11233-8; PMID:17581881; http://dx.doi.org/10.1073/pnas.0701045104
54. Cabezon E, Butler PJ, Runswick MJ, Walker JE. Modulation of the oligomerization state of the bovine F1-ATPase inhibitor protein, IF1, by pH. J Biol Chem 2000; 275:25460-4; PMID:10831597; http://dx.doi.org/10.1074/jbc.M003859200
55. Bason JV, Runswick MJ, Fearnley IM, Walker JE. Binding of the inhibitor protein IF(1) to bovine F(1)-ATPase. J Mol Biol 2011; 406:443-53; PMID:21192948; http://dx.doi.org/10.1016/j.jmb.2010.12.025
56. Wilkens S, Capaldi RA. ATP synthase's second stalk comes into focus. Nature 1998; 393:29; PMID:9590688; http://dx.doi.org/10.1038/29908
57. Dickson VK, Silvester JA, Fearnley IM, Leslie AG, Walker JE. On the structure of the stator of the mitochondrial ATP synthase. EMBO J 2006; 25:2911-8; PMID:16791136; http://dx.doi.org/10.1038/sj.emboj.7601177
58. Stewart AG, Lee LK, Donohoe M, Chaston JJ, Stock D. The dynamic stator stalk of rotary ATPases. Nature communications 2012; 3:687
59. Oot RA, Huang LS, Berry EA, Wilkens S. Crystal structure of the yeast vacuolar ATPase heterotrimeric EGC(head) peripheral stalk complex. Structure 2012; 20:1881-92; PMID:23000382; http://dx.doi.org/10.1016/j.str.2012.08.020
60. Del Rizzo PA, Bi Y, Dunn SD. ATP synthase b subunit dimerization domain: a right-handed coiled coil with offset helices. J Mol Biol 2006; 364:735-46; PMID:17028022; http://dx.doi.org/10.1016/j.jmb.2006.09.028
61. Parry DA, Fraser RD, Squire JM. Fifty years of coiled-coils and α-helical bundles: a close relationship between sequence and structure. J Struct Biol 2008; 163:258-69; PMID:18342539; http://dx.doi.org/10.1016/j.jsb.2008.01.016
62. Stetefeld J, Jenny M, Schulthess T, Landwehr R, Engel J, Kammerer RA. Crystal structure of a naturally occurring parallel right-handed coiled coil tetramer. Nat Struct Biol 2000; 7:772-6; PMID:10966648; http://dx.doi.org/10.1038/79006
63. Kühnel K, Jarchau T, Wolf E, Schlichting I, Walter U, Wittinghofer A, et al. The VASP tetramerization domain is a right-handed coiled coil based on a 15-residue repeat. Proc Natl Acad Sci U S A 2004; 101:17027-32; PMID:15569942; http://dx.doi.org/10.1073/pnas.0403069101
64. Stewart AG, Stock D. Priming a molecular motor for disassembly. Structure 2012; 20:1799-800; PMID:23141690; http://dx.doi.org/10.1016/j.str.2012.10.003
65. Baker LA, Watt IN, Runswick MJ, Walker JE, Rubinstein JL. Arrangement of subunits in intact mammalian mitochondrial ATP synthase determined by cryo-EM. Proc Natl Acad Sci U S A 2012; 109:11675-80; PMID:22753497; http://dx.doi.org/10.1073/pnas.1204935109
66. Davies KM, Anselmi C, Wittig I, Faraldo-Gómez JD, Kühlbrandt W. Structure of the yeast F1Fo-ATP synthase dimer and its role in shaping the mitochondrial cristae. Proc Natl Acad Sci U S A 2012; 109:13602-7; PMID:22864911; http://dx.doi.org/10.1073/pnas.1204593109
67. Vonck J, Pisa KY, Morgner N, Brutschy B, Müller V. Three-dimensional structure of A1A0 ATP synthase from the hyperthermophilic archaeon Pyrococcus furiosus by electron microscopy. J Biol Chem 2009; 284:10110-9; PMID:19203996; http://dx.doi.org/10.1074/jbc.M808498200
68. Lau WC, Rubinstein JL. Subnanometre-resolution structure of the intact Thermus thermophilus H+-driven ATP synthase. Nature 2012; 481:214-8; PMID:22178924; http://dx.doi.org/10.1038/nature10699
69. Kitagawa N, Mazon H, Heck AJ, Wilkens S. Stoichiometry of the peripheral stalk subunits E and G of yeast V1-ATPase determined by mass spectrometry. J Biol Chem 2008; 283:3329-37; PMID:18055462; http://dx.doi.org/10.1074/jbc.M707924200
70. Kane PM. Disassembly and reassembly of the yeast vacuolar H(+)-ATPase in vivo. J Biol Chem 1995; 270:17025-32; PMID:7622524
71. Smardon AM, Kane PM. RAVE is essential for the efficient assembly of the C subunit with the vacuolar H(+)-ATPase. J Biol Chem 2007; 282:26185-94; PMID:17623654; http://dx.doi.org/10.1074/jbc.M703627200
72. Muench SP, Huss M, Song CF, Phillips C, Wieczorek H, Trinick J, et al. Cryo-electron microscopy of the vacuolar ATPase motor reveals its mechanical and regulatory complexity. J Mol Biol 2009; 386:989-99; PMID:19244615; http://dx.doi.org/10.1016/j.jmb.2009.01.014
73. Benlekbir S, Bueler SA, Rubinstein JL. Structure of the vacuolar-type ATPase from Saccharomyces cerevisiae at 11-Å resolution. Nat Struct Mol Biol 2012; 19:1356-62; PMID:23142977; http://dx.doi.org/10.1038/nsmb.2422
74. Pietrement C, Sun-Wada GH, Silva ND, McKee M, Marshansky V, Brown D, et al. Distinct expression patterns of different subunit isoforms of the V-ATPase in the rat epididymis. Biol Reprod 2006; 74:185-94; PMID:16192400; http://dx.doi.org/10.1095/biolreprod.105.043752
75. Sugawa M, Okada KA, Masaike T, Nishizaka T. A change in the radius of rotation of F1-ATPase indicates a tilting motion of the central shaft. Biophys J 2011; 101:2201-6; PMID:22067159; http://dx.doi.org/10.1016/j.bpj.2011.09.016
76. van Roon H, van Breemen JF, de Weerd FL, Dekker JP, Boekema EJ. Solubilization of green plant thylakoid membranes with n-dodecyl-alpha,D-maltoside. Implications for the structural organization of the Photosystem II, Photosystem I, ATP synthase and cytochrome b6 f complexes. Photosynth Res 2000; 64:155-66; PMID:16228454; http://dx.doi.org/10.1023/A:1006476213540

77. Giraud MF, Paumard P, Sanchez C, Brethes D, Velours J, Dautant A. Rotor architecture in the yeast and bovine F(1)-c-ring complexes of F-ATP synthase. J Struct Biol 2012; 177:490-7; PMID:22119846; http://dx.doi.org/10.1016/j.jsb.2011.10.015
78. Boyer PD. The ATP synthase--a splendid molecular machine. Annu Rev Biochem 1997; 66:717-49; PMID:9242922; http://dx.doi.org/10.1146/annurev.biochem.66.1.717
79. Pogoryelov D, Yildiz O, Faraldo-Gómez JD, Meier T. High-resolution structure of the rotor ring of a proton-dependent ATP synthase. Nat Struct Mol Biol 2009; 16:1068-73; PMID:19783985; http://dx.doi.org/10.1038/nsmb.1678